

Real-time particle tracking at 10,000 fps using optical fiber illumination

Oliver Otto,¹ Fabian Czerwinski,² Joanne L. Gornall,¹ Gunter Stober,³
Lene B. Oddershede,² Ralf Seidel,⁴ and Ulrich F. Keyser^{1,*}

¹*Cavendish Laboratory, University of Cambridge, J. J. Thomson Avenue,
Cambridge CB3 0HE, UK*

²*Niels Bohr Institute, Blegdamsvej, 2100 Copenhagen, Denmark*

³*Leibniz-Institute of Atmospheric Physics, Rostock University, Schlosstr. 6,
18225 Kühlungsborn, Germany*

⁴*Biotechnological Center, TU Dresden, Tatzberg 47-51, 01307 Dresden, Germany*

[*ufk20@cam.ac.uk](mailto:ufk20@cam.ac.uk)

Abstract: We introduce optical fiber illumination for real-time tracking of optically trapped micrometer-sized particles with microsecond time resolution. Our light source is a high-radiance mercury arc lamp and a 600 μm optical fiber for short-distance illumination of the sample cell. Particle tracking is carried out with a software implemented cross-correlation algorithm following image acquisition from a CMOS camera. Our image data reveals that fiber illumination results in a signal-to-noise ratio usually one order of magnitude higher compared to standard Köhler illumination. We demonstrate position determination of a single optically trapped colloid with up to 10,000 frames per second over hours. We calibrate our optical tweezers and compare the results with quadrant photo diode measurements. Finally, we determine the positional accuracy of our setup to 2 nm by calculating the Allan variance. Our results show that neither illumination nor software algorithms limit the speed of real-time particle tracking with CMOS technology.

© 2010 Optical Society of America

OCIS codes: (000.3110) Instruments, apparatus, and components common to the sciences; (060.2310) Fiber optics; (030.4280, 110.4280) Noise in imaging systems; (100.2960) Image analysis; (140.7010) Laser trapping; (230.5170) Photodiodes; (120.4800, 350.4800) Optical standards and testing; (350.4855) Optical tweezers or optical manipulation.

References and links

1. K. Bacia, S. A. Kim, and P. Schuille, "Fluorescence cross-correlation spectroscopy in living cells," *Nat. Methods* **3**, 83–89 (2006).
2. E. Betzig, G. H. Patterson, R. Sougrat, O. W. Lindwasser, S. Olenych, J. S. Bonifacino, M. W. Davidson, J. Lippincott-Schwartz, and H. F. Hess, "Imaging intracellular fluorescent proteins at nanometer resolution," *Science* **313**, 1642–1645 (2006).
3. M. K. Cheezum, W. F. Walker, and W. H. Guilford, "Quantitative Comparison of Algorithms for Tracking Single Fluorescent Particles," *Biophys. J.* **81**, 2378–2388 (2001).
4. U. F. Keyser, B. N. Koeleman, S. van Dorp, D. Krapf, R. M. M. Smeets, S. G. Lemay, N. H. Dekker, and C. Dekker, "Direct force measurements on DNA in a solid-state nanopore," *Nat. Phys.* **2**, 473–477 (2006).
5. H. Salman, D. Zbaida, Y. Rabin, D. Chatenay, and M. Elbaum, "Kinetics and mechanism of DNA uptake into the cell nucleus," *Proc. Natl. Acad. Sci. USA* **98**, 7247–7252 (2001).
6. J. Wen, L. Lancaster, C. Hodges, A. Zeri, S. H. Yoshimura, H. F. Noller, C. Bustamante, and I. Tinoco, "Following translation by single ribosomes one codon at a time," *Nature* **452**, 598–603 (2008).

7. A. Ashkin, "Acceleration And Trapping Of Particles By Radiation Pressure," *Phys. Rev. Lett.* **24**, 156–159 (1970).
8. G. M. Gibson, J. Leach, S. Keen, A. J. Wright, and M. J. Padgett, "Measuring the accuracy of particle position and force in optical tweezers using high-speed video microscopy," *Opt. Express* **16**, 14561–14570 (2008).
9. K. C. Neuman and S. M. Block, "Optical trapping," *Rev. Sci. Instrum.* **75**, 2787–2809 (2004).
10. J. E. Curtis, B. A. Koss, and D. G. Grier, "Dynamic holographic optical tweezers," *Opt. Commun.* **207**, 169–175 (2002).
11. F. C. Cheong, B. J. Krishnatreya, and D. G. Grier, "Strategies for three-dimensional particle tracking with holographic video microscopy," *Opt. Express* **18**, 13563–13573 (2010).
12. A. van der Horst and N. R. Forde, "Power spectral analysis for optical trap stiffness calibration from high-speed camera position detection with limited bandwidth," *Opt. Express* **18**, 7670–7677 (2010).
13. O. Otto, C. Gutsche, F. Kremer, and U. F. Keyser, "Optical tweezers with 2.5 kHz bandwidth video detection for single-colloid electrophoresis," *Rev. Sci. Instrum.* **79**, 023710 (2008).
14. S. Keen, J. Leach, G. Gibson, and M. J. Padgett, "Comparison of a high-speed camera and a quadrant detector for measuring displacements in optical tweezers," *J. Opt. A, Pure Appl. Opt.* **9**, 264–266 (2007).
15. R. Bowman, G. Gibson, and M. Padgett, "Particle tracking stereomicroscopy in optical tweezers: control of trap shape," *Opt. Express* **18**, 11785–11790 (2010).
16. M. Towrie, S. W. Botchway, A. Clark, E. Freeman, R. Halsall, A. W. Parker, M. Prydderch, R. Turchetta, A. D. Ward, and M. R. Pollard, "Dynamic position and force measurement for multiple optically trapped particles using a high-speed active pixel sensor," *Rev. Sci. Instrum.* **80**, 103704 (2009).
17. P. L. Biancaniello and J. C. Crocker, "Line optical tweezers instrument for measuring nanoscale interactions and kinetics," *Rev. Sci. Instrum.* **77**, 113702 (2006).
18. G. M. Hale and M. R. Querry, "Optical Constants of Water in the 200-nm to 200-micrometer Wavelength Region," *Appl. Opt.* **12**, 555–563 (1973).
19. Y. Liu, D. K. Cheng, G. J. Sonek, M. W. Berns, C. F. Chapman, and B. J. Tromberg, "Evidence for localized cell heating induced by infrared optical tweezers," *Biophys. J.* **68**, 2137–2144 (1995).
20. U. F. Keyser, D. Krapf, B. N. Koeleman, R. M. M. Smeets, N. H. Dekker, and C. Dekker, "Nanopore tomography of a laser focus," *Nano Lett.* **5**, 2253–2256 (2005).
21. I. Semenov, O. Otto, G. Stober, P. Papadopoulos, U. F. Keyser, and F. Kremer "Single colloid electrophoresis," *J. Colloid Interface Sci.* **337**, 260–264 (2009).
22. F. Czerwinski, A. C. Richardson, and L. B. Oddershede, "Quantifying Noise in Optical Tweezers by Allan Variance," *Opt. Express* **17**, 13255–13269 (2009).
23. F. Czerwinski and L. B. Oddershede, "TIMESERIESSTREAMING.VI: LabVIEW program for reliable data streaming of large analog time series," *Comput. Phys. Commun.* accepted for publication (2010).
24. K. Berg-Sørensen and H. Flyvbjerg, "Power spectrum analysis for optical tweezers," *Rev. Sci. Instrum.* **75**, 594–612 (2004).
25. C. Gosse and V. Croquette, "Magnetic Tweezers: Micromanipulation and Force Measurement at the Molecular Level," *Biophys. J.* **82**, 3314–3329 (2002).
26. O. Otto, J. L. Gornall, G. Stober, F. Czerwinski, R. Seidel, and U. F. Keyser, "High-Speed Video-Based Tracking of Optically Trapped Colloids," *J. Opt. A, Pure Appl. Opt.* accepted for publication (2010).
27. M. Andersson, F. Czerwinski, and L. B. Oddershede, "Allan variance for optimizing optical tweezers calibration," under review (2010).
28. F. Czerwinski, A. C. Richardson, C. Selhuber-Unkel, and L. B. Oddershede, "Allan Variance Analysis as Useful Tool to Determine Noise in Various Single-Molecule Setups," *Proc. SPIE* **7400**, 740004 (2009).
29. W. P. Wong and K. Halvorsen, "The effect of integration time on fluctuation measurements: calibrating an optical trap in the presence of motion blur," *Opt. Express* **14**, 12517–12531 (2006).

1. Introduction

Light microscopy is one of the most versatile and successful measurement techniques providing accurate spatial and temporal information of particle movements [1]. One prominent example is the tracking of single fluorophores or whole organelles in living cells to clarify cellular processes *in vivo* [2, 3]. On the molecular level, optical tweezers offer the opportunity to characterize and monitor mechanical properties of single DNA or protein molecules in aqueous environments [4–6]. Only a few decades after their introduction, optical tweezers are now a widely used tool in physics and biology [7]. Optical tweezers can exert piconewton forces on micron-sized objects like colloidal particles while measuring the resulting displacements with sub-nanometer accuracy [8]. Two main routes are followed to measure the motion of the trapped particle, namely photo diodes and video-based particle tracking [9]. While photo diodes

are suited for position detection of a single colloid, they are not ideal for applications like holographic optical tweezers because monitoring of multiple colloids is complicated [10, 11]. In contrast, video-based particle tracking is capable of following several colloids in the field of view at the same time [12]. The progress in the development of new cameras and illumination systems has made it possible to extend the acquisition speed of this tracking method to the millisecond timescale [13–15]. However, this technology is obviously limited by the number of photons that can be recorded by the CCD or CMOS camera per particle.

Recently, several groups have investigated and improved the speed and illumination techniques for single particle tracking in optical tweezers. Gibson *et al.* demonstrated video-based position determination of colloids in optical tweezers using a CMOS camera and standard desktop PC. They recorded particle positions at 1,000 frames per second (fps) in real-time and were only limited by the brightness of their tungsten-halogen lamp [8]. Using a 100 W halogen light source Keen *et al.* showed image acquisition at 2,000 fps but were restricted by the buffer size of their camera to measurement times of 4 s [14]. Van der Horst *et al.* increased the threshold in video-based position determination to 2,500 fps but were ultimately limited by the light intensity [12]. Otto *et al.* carried out experiments on single colloids in optical traps using a CMOS camera and standard software environment [13]. At acquisition rates of 5,000 fps their measurement time was limited by the size of the pre-allocated memory, only. By developing a novel pixel sensor in combination with data analysis based on field programmable gate array (FPGA) circuits Towrie *et al.* determined the position of 6 colloids simultaneously [16]. Their system allows for frame rates up to 15,000 fps but is ultimately restricted by the brightness of their standard light source. Biancaniello *et al.* overcame these limitations by introducing laser illumination into an optical tweezers setup allowing for video-based off-line position tracking with 10 kHz bandwidth [17]. Although lasers are the ultimate high brightness light source accompanying effects like coherence and collimation challenge the alignment of the optical setup.

In this paper, we describe an optical tweezers setup which is based on a novel optical fiber illumination approach and CMOS camera based particle tracking. We demonstrate that a combination of this fiber-based light-source and an entirely software implemented tracking algorithm is sufficient to follow the fluctuations of single or multiple particles at up to 10,000 fps in real-time and over the duration of hours. The quality of the optical fiber illumination is assessed by comparing the images of optically trapped colloids with those obtained in a traditional Köhler illumination alignment. We determine the signal-to-noise ratios (SNR) and show that optical fiber illumination allows for measurements at 40,000 fps with a high SNR of 10. Characterization of the optical trap and determination of the optimal measurement time is carried out using an optimized calibration protocol including Allan variance and power spectral density analysis of time series. We utilize this protocol for data obtained from CMOS measurements comparing Köhler illumination and optical fiber illumination as well as for CCD and quadrant photo diode (QPD) recordings. We show that CMOS-based position tracking allows us to measure close to the thermal limit while giving almost the same accuracy as data obtained from a QPD detector.

2. Materials and methods

2.1. Optical tweezers setup

In our optical tweezers setup (Fig. 1) the beam of an Ytterbium fiber laser (YLM-5-LP, IPG Laser, Germany) is expanded to approximately 7.2 mm, and coupled into the back aperture of a water-immersion microscope objective (UPlanSApo/IR, 60 \times , NA=1.20, Olympus, Japan). The diffraction limited spot forms a static optical trap inside a fluidic cell. At the chosen wavelength, the absorption coefficient of water is small, reducing laser induced heating to approximately 1.5 K per 100 mW [18–20]. The fluidic cell itself consists of a 100 μ m thick cover slip and a

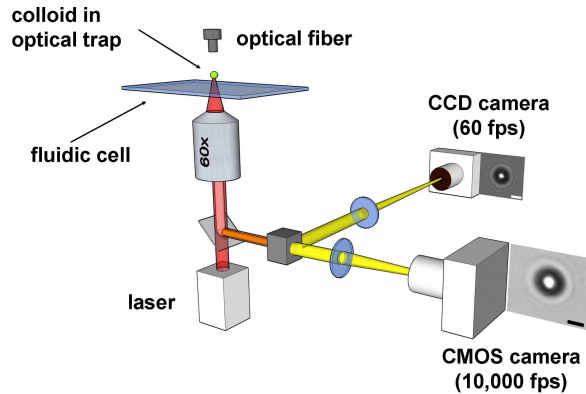


Fig. 1. Schematic drawing of the custom built optical tweezers setup. The 1064 nm laser is focused into a fluidic cell by a 60x water immersion objective. Collimated light of a mercury arc lamp (not shown) illuminates the region of interest through an optical fiber. A high-speed CMOS camera captures 10,000 frames per second and is used for position determination. A slower CCD with up to 60 frames per second is used to provide a full field of view. The length of the scale bars in the colloid images are $2\ \mu\text{m}$.

PMMA block, separated by a PDMS spacer. It is mounted onto an XYZ piezo nanopositioning stage (P-517.3, Physik Instrumente, Germany) connected to a digital piezo controller (E-710.3, Physik Instrumente, Germany). The nanopositioning stage enables multi-axis motion with a resolution of 1 nm and a range of $100\ \mu\text{m}$ in the x - and y -directions and $20\ \mu\text{m}$ in the z -direction.

For illuminating the Region of Interest (ROI) we follow a novel approach integrating a mercury arc lamp (100 W, LOT - Oriel, UK) and an optical fiber (600 μm core diameter multimode silica fiber, NA=0.39, Thorlabs, UK) into a modular and powerful light source. Our solution has some major advantages. The lamp housing is passively cooled and does not contribute to noise in the setup. With an arc size of only $250\ \mu\text{m}$ our 100 W lamp is a high-radiance source and produces very intense collimated beams. The light is focused onto the input of the optical fiber and is carried along by total internal reflection. Figure 1 shows the output of the fiber which is mounted on top of the sample cell by a custom-built adapter. The ROI is thus illuminated in transmission mode with an effective distance between light source and optically trapped colloid of less than 2 mm. Taking into account the numerical aperture of 0.39 the optical fiber illuminates an effective area of 1 mm diameter. Light diffracted by the colloid is imaged onto the camera by a tube lens with $f=20\ \text{cm}$ focal length. We estimate an effective light power over the $100 \times 100\ \text{pixels}^2$ (px^2) ROI of approximately $1\ \mu\text{W}$.

All experiments are carried out with polystyrene colloids of diameter $(3.27 \pm 0.32)\ \mu\text{m}$ (Kisker, Germany) in deionized water. The region of interest around a colloid is monitored by a CMOS camera (MC1362, Mikrotrotron, Germany) and a high performance frame-grabber card (NI PCIe-1429, National Instruments, UK) [9, 13, 21].

A second optical tweezers setup from Czerwinski *et al.* described in [22] is used to validate the results obtained from our CMOS-based position tracking. In contrast to our system shown in Fig. 1, Czerwinski *et al.* measure the forward scattered light from a colloid applying a quadrant photo diode (S5981, Hamamatsu, Japan) and a CCD camera (Pike-100 B, Allied Vision Technologies, USA) [23].

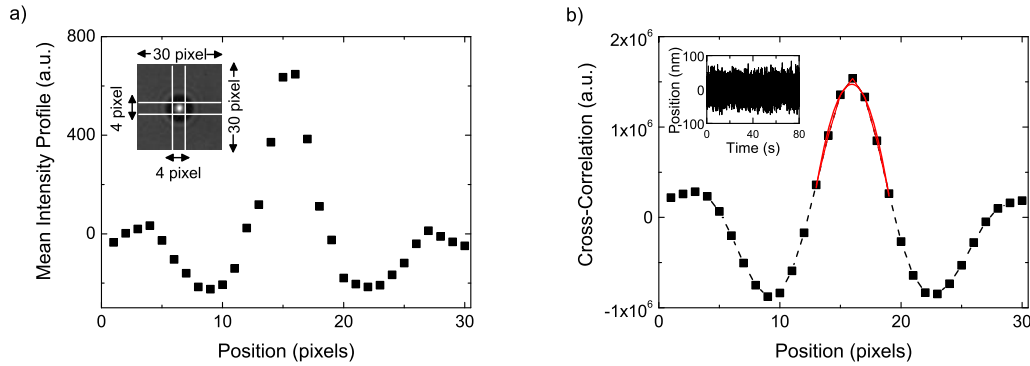


Fig. 2. Implementation of the position tracking algorithm. (a) The graph shows the mean intensity profile along an $4 \times 30\text{px}^2$ rectangular array of the $30 \times 30\text{px}^2$ sub-ROI (inset). The intensity profile is calculated in x - and y - direction independently. (b) 1-dimensional cross-correlation transformation and 2^{nd} -order polynomial fit of $\pm 3\text{px}$ around the maxima. The inset shows a time trace for a colloid tracked for 80 s at 10,000 fps in real-time.

2.2. Tracking algorithm and implementation

We aim to perform video-based position tracking of particles at temporal bandwidths previously only accessible to photodiode detector systems [24] or FPGA controlled cameras [16]. Therefore, our technique must be capable of simultaneous high-speed image acquisition and position tracking, in real-time. At the full resolution of $1280 \times 1024\text{px}^2$ our camera is specified to 500 frames per second. Based on the CMOS chip pixel size of $14\ \mu\text{m}$ we determine the resolution of our image system to $214\ \text{nm}/\text{pixel}$. By defining a ROI of smaller sizes ($100 \times 100\text{px}^2$) image acquisition faster than a few thousands frames per second can be easily achieved. This leaves as limiting step the number of photons arriving at the camera within the shutter time. The shortest shutter times used in this study were $20\ \mu\text{s}$.

Since the typical amplitude of the motion of a trapped colloid is of the order of tens of nanometers, position determination must be carried out for one or more particles with sub-pixel accuracy. Our position tracking algorithm uses cross-correlation analysis, described in [25]. The initial position is defined by the user within a sub-ROI of e.g. $30 \times 30\text{px}^2$ [inset Fig. 2(a)]. A rectangular array of pixels, $4 \times 30\text{px}^2$ in size, passing through the center of the sub-ROI, is binned and then normalized to give the mean intensity profiles for the x - and y -axes separately. Figure 2(a) shows this for the x -direction. To obtain sub-pixel accuracy, the cross-correlation of the mean intensity distribution with its reverse is calculated by applying the convolution theorem. The result is presented by the black dashed line in Fig. 2(b). Subsequently, the peak in the cross-correlation is fit with a second-order polynomial using seven points around the maximum value. The difference between the peak position and the center of the sub-ROI is used to calculate the relative displacement of the colloid. In the inset of Fig. 2(b) we show the positions of an optically trapped colloid calculated by the above algorithm for a 80 seconds time trace tracked at 10,000 fps in real-time.

We developed our acquisition software in LabVIEW (National Instruments, Austin, TX, USA) and C/C++. Image recording, tracking and streaming are done in a highly parallelized manner, directly assigned to two different CPU cores. Communication between timed loops is achieved by queues. Streaming of the tracked positions is done into the RAM and subsequently onto the hard disk. A block diagram of our LabVIEW software can be found in the supplementary material. We tested continuous acquisition over one hour at 10,000 fps. There was

virtually no limitation but disk space. We also benchmarked our software implemented tracking algorithm by monitoring the lost frames in a time trace. A frame is considered to be lost if the colloid position had not been calculated before the subsequent frame was acquired. In long-term measurements at 10,000 fps we found less than 5 missing frames for every 100,000 frames recorded, i.e. 0.005 %.

2.3. Calibration and accuracy measurements

The optical trap was calibrated by analyzing the Brownian fluctuations of a confined polystyrene colloid in deionized water. We use the power spectral density method [24] within a recently suggested optimized calibration protocol [26,27]. In this protocol we take a time trace and derive the Allan variance $\sigma_x^2(\tau)$ [22]:

$$\sigma_x^2(\tau) = \frac{1}{2} \left\langle (x_{i+1} - x_i)^2 \right\rangle_\tau, \quad (1)$$

where one calculates the average of the differences between the means of neighboring intervals x_i of measurement time τ . The Allan deviation is a function of time and allows the positional accuracy to be determined for any given τ . The absolute minimum denotes the optimal measurement time for calibration τ_{calib} [22].

Subsequently, we split the time trace into intervals of τ_{calib} , calculate the power spectral density (PSD) of each and derive the averaged PSD. It reveals the Lorentzian profile for the frequency spectrum of an object in an harmonic potential:

$$S(f) = \frac{k_B T}{\gamma \pi^2 (f_c^2 + f^2)}, \quad (2)$$

where k_B is the Boltzmann constant and T the temperature. For the drag coefficient γ we assume Stokes drag for a sphere with radius r moving in a fluid with viscosity η :

$$\gamma = 6\pi\eta r. \quad (3)$$

We use $\eta = 8.9 \cdot 10^{-4} \text{ Pa} \cdot \text{s}$ for measurements in water. The trap stiffness k_{trap} is directly proportional to the corner frequency f_c :

$$k_{\text{trap}} = 2\pi\gamma f_c. \quad (4)$$

To determine the corner frequency f_c , and consequently the trap stiffness k_{trap} , the power spectrum is integrated numerically and the resulting arctangent function is fit using the least-square method. An example of this is given in the inset of Fig. 5 for a laser power of 100 mW. Only frequencies between $f_{\text{min}} = 10 \text{ Hz}$ and $f_{\text{max}} = 500 \text{ Hz}$, are considered. Keeping these fitting parameters constant for all acquisition rates allows for quantitative comparison of the derived corner frequencies. Each fit is corrected for possible aliasing effects according to Ref. [24].

Knowing the trap stiffness, a thermal limit for the accuracy of the particle position averaged over the time period τ_{calib} is given by [8]:

$$SE_{(x)} \approx \sqrt{\frac{2k_B T \gamma}{k_{\text{trap}}^2 \tau}}. \quad (5)$$

In principle, this limit sets the positional accuracy of a Brownian particle and is proportional to $\tau^{-0.5}$. Any experimental setup though is exposed to drift that typically increases the measured deviation following τ^c with $c \leq 1$. Therefore, drift becomes dominant beyond an optimal calibration time, and additional averaging accumulates only the drift response [22].

3. Results

3.1. Illumination

Video-based position tracking is ultimately limited by the number of photons recorded by the camera [9]. A decreasing shutter time and a correspondingly increasing frame rate usually leads to an increase of noise in the image due to the lower number of photons available per time interval. Consequently, the spatial resolution of the optical system is reduced. Measurements at high camera frame rates require high-radiance illumination and the position tracking algorithm to be stable over a wide range of exposure times [3].

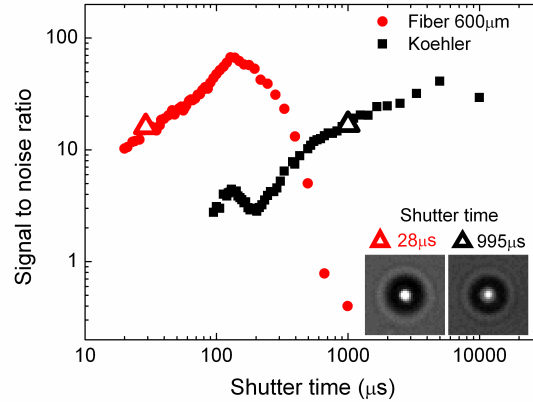


Fig. 3. Signal-to-noise ratio as a function of camera shutter time for illumination by $600\ \mu\text{m}$ optical fiber (red curve) and Köhler alignment (black curve). The inset shows CMOS images of colloids yielding the same signal-to-noise ratio of 16 at very different shutter times of $28\ \mu\text{s}$ (fiber illumination) and $995\ \mu\text{s}$ (Köhler illumination). The intensity of each light source was kept constant during the measurement.

One important index to quantify the quality of an image is the signal-to-noise ratio. Generally, it is defined as the mean intensity (μ_O) of the object divided by the root mean square noise of the background (σ_B) [3]. We extend the above definition by including a correction factor μ_R that covers image artefacts at very high light levels:

$$SNR = \frac{\mu_O - \mu_R}{\sigma_B}, \quad (6)$$

where σ_B is extracted from the background area not covered by an object. Diffraction of light by the optically trapped colloid creates an Airy pattern having a maximum of intensity in the center enclosed by a series of dark and bright concentric rings. Very long shutter times and overexposure of the image lead to the disappearance of the first minimum of the Airy disc and to an overestimation of the object intensity which results in an artificially high SNR. The correction factor μ_R is the mean intensity of this first concentric minimum. For short shutter times this correction factor has no effect as the area of the minimum is uniformly black and $\mu_R \rightarrow 0$. At long shutter times μ_R allows for correct consideration of effects due to overexposure and ensures that the number of pixels representing the maximum of the Airy disc remains constant.

Figure 3 compares the signal-to-noise ratio of images of optically trapped colloids illuminated by a $600\ \mu\text{m}$ optical fiber and a Köhler configuration respectively. All data were analyzed

for different shutter times using Eq. (6). The Köhler illumination curve yields a SNR maximum of 40 at $4,995\ \mu\text{s}$ (200 fps) and decreases towards a SNR minimum of 2 at $203\ \mu\text{s}$ (4,800 fps). The variations in SNR at very short shutter times originate from fluctuations in σ_B at low light levels. The maximum at $4,995\ \mu\text{s}$ however is due to overexposing of the images at longer shutter times at which the signal becomes constant while the background noise is still increasing.

The red curve in Fig. 3 shows the SNR for fiber illumination as a function of camera shutter time. It reveals qualitative similarities with data obtained from Köhler illumination but the SNR is generally one order of magnitude higher for comparable shutter times. The signal-to-noise ratio increases to a pronounced maximum of 67 at $128\ \mu\text{s}$ shutter time (7,500 fps) and decreases towards 10 at $20\ \mu\text{s}$ (40,000 fps). The maximum reflects again the influence of overexposure at long shutter times where background noise dominates the image and almost all pixels are saturated to the 8-bit peak value of 255 of our CMOS sensor.

The inset in Fig. 3 shows two colloid images both having a SNR of 16. The image taken with optical fiber illumination has a 35-times reduced exposure time compared to the Köhler illuminated image. Comparing both curves underlines the power of introducing intense light sources in an optical tweezers setup.

3.2. Comparison CCD, CMOS, and QPD

After determining the optimal illumination level, we monitor the Brownian motion of optically trapped polystyrene colloids at a laser power adjusted to a trap stiffness of $k_{\text{trap}} = (9.13 \pm 0.64) \frac{\text{pN}}{\mu\text{m}}$ for at least 130 s [Fig. 4(a)]. CMOS data was acquired at a frame rate of 6,000 fps. By using a separate experimental setup time traces based on position detection via QPD and CCD were recorded simultaneously at acquisition rates f_{acq} of 50 kHz and 60 fps respectively. The shutter time of the CCD camera was adjusted to 2.56 ms and for the CMOS camera to $162\ \mu\text{s}$. Drift quantification [Fig. 4(b)] and calibration (Fig. 5 inset) was performed as described in Section 2.3. The tracking resolution per video frame of our CMOS system is determined by adhering a colloid to the surface of our sample cell and moving the piezoelectric stage in 2 nm steps. Using the algorithm described above we can resolve these steps with 0.2 nm accuracy which is regarded as the error for the instantaneous colloid position (see supplementary material).

In addition to determine the optimal calibration time τ_{calib} we use Allan variance to quantify the positional accuracy in an assumption-free manner. In Fig. 4b, the Allan deviation is plotted as a function of measurement time. The dashed line represents the thermal limit Eq. (5). This thermal limit depends on the drag coefficient γ and the trap stiffness k_{trap} . The largest uncertainty of γ derives from the error in the radius of the sphere. The corner frequency is determined with a relative error of $\Delta f_c / f_c = 2\%$. Using Eqs. (3), (4) and (5), the error of the thermal limit becomes:

$$\frac{\Delta SE_{\langle x \rangle}}{SE_{\langle x \rangle}} = \sqrt{\left(\frac{\Delta f_c}{f_c}\right)^2 + \frac{1}{2}\left(\frac{\Delta r}{r}\right)^2} \approx 7.35\% . \quad (7)$$

We illustrate the impact of those uncertainties in the absolute errors of the thermal limit in Fig. 4(b). Data from CMOS-based detection stays close to the thermal limit and reaches a remarkable accuracy of 2 nm when positions are averaged over 3 s to 8 s measurement time. Beyond that drift becomes dominant and the Allan deviation clearly deviates from the thermal limit. QPD and CCD measurements were done on a separate setup having the trap stiffness adjusted to the same k_{trap} . The QPD follows the thermal limit up to tens of seconds. Due to its low sampling frequency, the CCD does not allow for measuring with positional accuracies at the thermal limit. This effect has been described before [28].

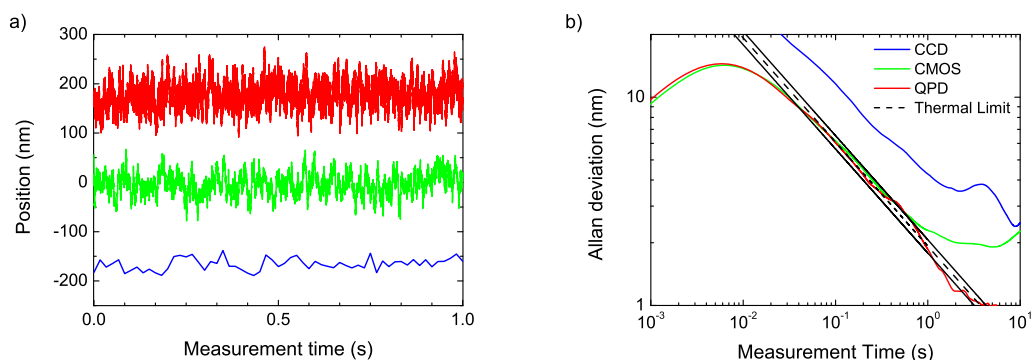


Fig. 4. (a) Time traces of a polystyrene colloid optically trapped in a harmonic potential with a corner frequency of about 47 Hz. Data from a CMOS camera (green) was acquired in an experiment at 6,000 fps. Fluctuations with a quadrant photodiode at 50 kHz (red) and a CCD camera at 60 fps (blue) were recorded simultaneously at a separate setup. For visualization the data was shifted along the y-axis. (b) Allan deviations of all time series in a) with a total length of 130 s each. The effect of aliasing causes the undersampled CCD data to be off the thermal limit by a factor of 3.

3.3. Stiffness over frame rate

Figure 5 summarizes calibration measurements with CMOS- and QPD-based particle tracking. The corner frequency was derived for various laser powers and camera frame rates. For video-based position determination two different sample illumination techniques were compared. The black data points in the lower frame rate interval between 500 fps and 6,000 fps show measurements where the colloid was illuminated with a cold-light source (150 W, Fiber Lite DC-950) in Köhler alignment. Calibration between 5,000 fps and 10,000 fps was carried out based on optical fiber illumination represented by the red data points in Fig. 5. Each data point is calculated from a set of measurements of 80,000 images each and analyzed as described above. The shutter time of the camera was kept constant at 162 μ s for Köhler and 95 μ s for fiber illumination.

Calibration was carried out at five different laser powers: 200 mW, 150 mW, 100 mW, 50 mW and 25 mW (top to bottom in Fig. 5). At a given laser power, the corner frequency is constant over a large range of camera frame rates, as expected. The transition zone between Köhler and optical fiber illumination shows the very same results for both techniques and allows to reliably access 100 μ s time resolution on a video-based tracking system. This proves that our system has sufficient bandwidth to calibrate stiff optical traps with high corner frequencies. For high laser powers and frame rates below 1,000 fps however, we see a deviation of f_c towards larger values. This effect can be explained by aliasing [29]. If the sampling rate approaches the corner frequency of the trapped colloid (under-sampling) high-frequency contributions of the power spectrum are folded back into low-frequency parts.

The stability of the optical system was confirmed by performing calibration using a quadrant photo diode at an separate optical tweezers setup. Particle tracking was done for 3.27 μ m polystyrene colloids at a laser power corresponding to the 200 mW video-based measurements. The frequency regime was set between 10 kHz and 500 kHz (blue data points). The data in Fig. 5 shows that the corner frequency values are in line with data from video-based particle tracking. This covers Köhler illumination and optical fiber illumination as well. In summary, our results show that CMOS-based calibration of optical tweezers not only approaches the sam-

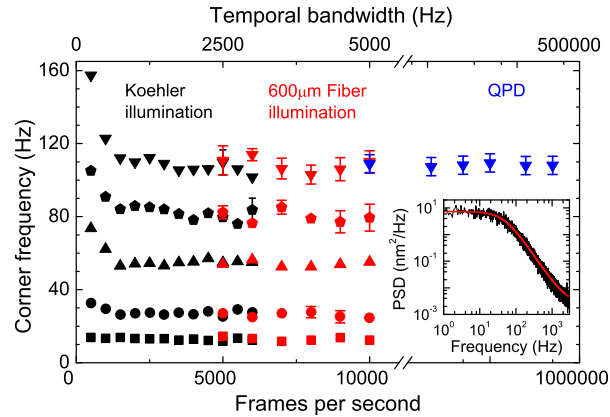


Fig. 5. Calibration of optical tweezers at different acquisition rates. Determination of corner frequency f_c was done at five different laser powers (top to bottom: 200 mW, 150 mW, 100 W, 50 mW, 25 mW) and compares results from Köhler (black) and 600 μm fiber (red) illumination respectively. At a separate setup an additional calibration with a quadrant photo diode (blue) was performed having the laser power adjusted to the video-based measurement. The error is calculated from a series of measurements and is given by the symbol size if not explicitly indicated on the graph. At given laser power the corner frequency remains constant with increasing camera frame rate. The deviation at low frame rates can be explained by aliasing effects of the recording. The shutter time of the CMOS camera was adjusted to 162 μs (Köhler illumination) and 95 μs (optical fiber illumination). The inset shows how the corner frequency f_c was obtained by power spectrum analysis of a confined colloid by numerically integrating the averaged PSD and fitting the resulting curve with an arctangent function. The corresponding time trace was recorded with the CMOS camera at 6,000 fps for 130 seconds.

pling rate of QPD systems but can give the same accuracy and stability in results.

In contrast to QPDs, cameras allow for tracking of multiple particle positions in parallel. There are only two limiting factors: The field of view of the camera sensor and the performance of the data analysis algorithm. Applying the techniques introduced in this paper we are able to synchronously track the position of two colloids at 6,000 fps in real-time (not shown).

4. Discussion

Precise position tracking of an optically trapped colloid requires high spatial and temporal accuracy to be combined in one detection system. This can be achieved by two methods. Quadrant photo diodes measure the particle induced deflection of laser light with a frequency of up to 500 kHz and allow for fluctuation analysis on a microseconds time scale. However, a single QPD can only monitor the position of one colloid at the same time and is therefore not directly suitable for e.g. holographic optical tweezers.

By integrating a novel optical fiber illumination technique into our optical tweezers setup we extend the effective application range of video-based particle tracking into the microseconds time scale. Light from a 100 W high-radiance mercury arc light source is coupled into a 600 μm fiber and guided directly to our sample cell. This alignment reduces the effective distance between light source and optically trapped colloid to approximately 2 mm. In contrast to laser illumination, we do not need any additional optics to correct for interference effects as the light from a mercury arc lamp is incoherent [17].

We demonstrate position tracking of a single colloid with frame rates up to 10,000 fps in real-time based on a purely software implemented cross-correlation algorithm and following image acquisition from a CMOS camera [26]. In addition, we extend our algorithm for multiple particles and demonstrate tracking of two colloids at 6,000 fps in parallel. Compared to hardware implemented algorithms our design allows for flexibility and full control by the user [16]. Our software takes advantage of multi-core programming and is implemented in a highly parallel manner. Based on these concepts we can perform high-speed video tracking for hours. In fact, the current restrictions of real-time position determination of a single colloid are only originated from the LabVIEW data processing rate. Using off-line data acquisition only, our setup allows for position tracking at frame rates up to 40,000 fps.

We assess the quality of our novel optical fiber illumination technique by calculating the signal-to-noise ratio of a colloid image at different shutter times of our camera. We compare the results with additional measurements obtained from Köhler illumination. Cheezum *et al.* calculate the limiting SNR for cross-correlation based position detection to 6 [3]. Our data shown in Fig. 3 reveals that the signal-to-noise ratio of fiber illuminated colloids is always well above 10 for shutter times between $20\ \mu\text{s}$ and $395\ \mu\text{s}$. Indeed, for measurements on the microseconds time scale corresponding to frame rates between 10,000 fps and 40,000 fps the SNR of fiber illumination is always one order of magnitude higher compared to Köhler illumination.

We characterize our optical trapping and tracking system by calculating the Allan deviation of a 6,000 fps CMOS time trace and compare our findings with 60 fps CCD and 50 kHz QPD data from a separate optical tweezers setup. Both, CMOS and QPD allow to measure close to the thermal limit for times up to several seconds. Our CMOS system reaches a remarkable positional accuracy of 2 nm even for weak traps. Allan variance analysis points out the stability of the two optical setups. Even for low trap stiffnesses, they were not significantly exposed to drift until 8 s, which was found to be the optimal calibration interval at those settings. Our tracking method assures long-term stability of positional bandwidth which to our knowledge has not been achieved by any other video-based setup so far.

We calibrate our optical trap by power spectrum analysis. The corner frequency depends linearly on the applied laser power, as expected. We perform these measurements for Köhler illumination, $600\ \mu\text{m}$ fiber illumination and position detection via QPD using two different optical tweezers setups. At fixed laser power Fig. 5 shows consistent results for measurements carried out using both position detection techniques. Further, we prove that the acquisition rate of the camera does not influence the tracking algorithm and that the trap stiffness is essentially independent from the selected illumination method.

5. Conclusion

We have demonstrated the application of novel optical fiber illumination in an optical tweezers setup that allows to study colloidal fluctuations on a microsecond time scale. Particle tracking is carried out video-based in real-time using an entirely software implemented cross-correlation algorithm in a standard desktop environment. The optical fiber illumination allows for image acquisition having signal-to-noise ratios well above 10 even for $20\ \mu\text{s}$ exposure times. We demonstrate CMOS-based position tracking of a single colloid with frame rates up to 10,000 fps over hours. In contrast to QPD measurements, we can straight forward study multiple particles in parallel at high bandwidth. Allan variance calculations are used to determine the positional accuracy of our setup to be about 2 nm. We use separate QPD experiments to validate our results. In summary, we demonstrate that optical fiber illumination in combination with video tracking is applicable for position determination close to sampling rates of QPD systems while yielding the same results, accuracy and stability.

Acknowledgments

U. F. Keyser and R. Seidel acknowledge funding by the Emmy Noether-Program of the DFG. O. Otto thanks for the PhD fellowship and support provided by the Boehringer Ingelheim Fonds. J. Gornall is supported by a Nanoscience E+ grant. L. B. Oddershede acknowledges support from the KU excellence program.